A Tutorial on Microwave Photonics

Jianping Yao, Microwave Photonics Research Laboratory, School of Electrical Engineering and Computer Science, University of Ottawa, Ottawa, Ontario, Canada K1N 6N5

Abstract: The broad bandwidth and low loss offered by modern photonics have led to an ever-increasing interest in the design and implementation of photonically assisted systems for the generation, processing, control and distribution of microwave signals, an area called microwave photonics. In this article, a tutorial on microwave photonics is presented with an emphasis on photonic true-time delay beamforming, radio-over-fiber and UWB-over-fiber distribution and photonic analog-to-digital conversion.

Introduction

A tutorial on microwave photonics with an emphasis on the photonic generation of microwave signals and photonic processing of microwave signals was presented recently [1]. In general, the microwave photonics techniques cover the following topics: 1) photonic generation of microwave signals, 2) photonic processing of microwave signals, 3) photonic distribution of microwave signals, and 4) photonic analog-to-digital conversion. In this article, the topics including photonic true-time delay beamforming, radio-over-fiber and UWB-over-fiber and photonics analog-to-digital conversion will be discussed.

Photonic True-Time Delay Beamforming

Phased array antennas (PAA) are playing an important role in modern radar, sonar and wireless communication systems. Conventional phased array antennas are realized based on electrical phase shifters, which suffer from the well-known beam squint problem, limiting the phase array antennas for narrowband operations. For many applications, however, it is highly desirable that the phase array antennas can operate in a broad band. An effective solution is to use true-time delay beamforming.

Squint Phenomenon

The squint phenomenon is characterized by the position of the main lobe of the array factor being oriented at different angles for different microwave frequencies. In other words, the energy associated with different frequencies is oriented in different directions and thus restricts the use of the antenna for narrowband applications only.

As can be seen from Fig. 1(a), to steer the beam to a direction with angle of θ relative to the broadside direction, a phase shifter with a phase shift of $\Delta\phi$ is required, which is given

$$\Delta\phi = 2\pi\frac{\Delta L}{\lambda} = 2\pi\frac{d\sin\theta}{\lambda} \tag{1}$$

The beam pointing direction is then given by

$$\theta = \sin^{-1}\left(\frac{\lambda}{2\pi d}\Delta\phi\right) \tag{2}$$

As can be seen the beam pointing direction is a function of the microwave wavelength or frequency. Therefore, a beamforming system using electronic phase shifters will only support narrowband operation or the beam will be corrupted, a phenomenon called *beam squint*. The problem can be solved if the phase shifter is replaced by a true-time delay line, as shown in Fig. 1(b), where a true-time delay line with a length of $\Delta L = d\sin\theta$ is used. The beam pointing direction is now given by

$$\theta = \sin^{-1}\left(\frac{\Delta L}{d}\right) \tag{3}$$

It can be seen that the beam pointing direction is independent of the microwave frequency. A wide instantaneous bandwidth operation that is squint free is ensured. Fig. 1(c) shows the beam squint effect for a phased array antenna using electronic phase shifters operating at a frequency band of 10–20 GHz. The far-field radiation pattern of the array factor for the frequency band between 10 and 20 GHz clearly shows that the orientation of the main lobe varies with the feed signal frequency. This phenomenon decreases significantly the performance of the beamforming system. Fig. 1(d) shows the array factor by using true-time delay components. The far-field radiation pattern of the array factor for the frequency band between 10 and 20 GHz clearly shows that the orientation of the main lobe does not vary with the feed signal frequency.

Photonic True-Time Delay Beamforming

Traditionally, feed networks and phase shifters for phased array antennas were realized using electronic components. As ever increasing requirement for performance, severe limitations were observed in electronic devices. For example, copper wires exhibit high losses at high frequencies resulting in a limited bandwidth for the feed signals. Furthermore, electronic beamforming networks have a relatively high weight, thus limiting their use in airborne and satellite systems. Optical components, with key advantages such as immunity to electromagnetic interference (EMI), low loss, small size and light weight, are being considered as a promising alternative for wideband phased array antennas.

True-time delay beamforming based on photonic technologies has been extensively investigated with the systems implemented based either on free-space optics [2] or fiber or guided-wave optics. A true-time delay beamforming system based on free space optics has a relatively large size and heavy weight. Most of the reported systems were implemented based fiber optics. The realization of tunable true-time delays based on a

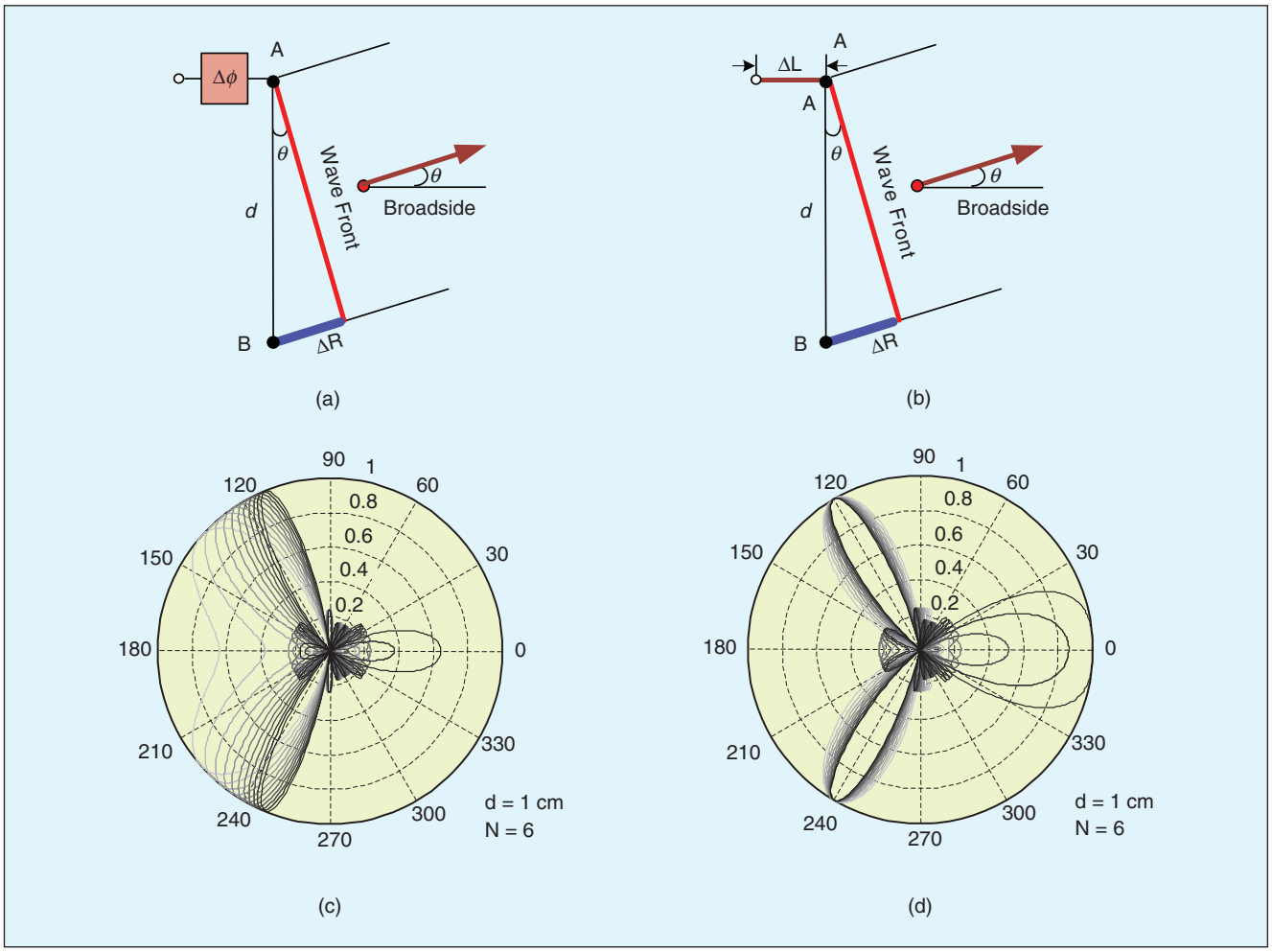

Figure 1. Beam steering (a) using a phase shifter, (b) using a delay line. (c) Beam squint effect for a phased array antenna operating at 10–20 GHz using electronic phase shifters. (d) Array factor of a phased array antenna operating at 10–20 GHz using true-time delay components.

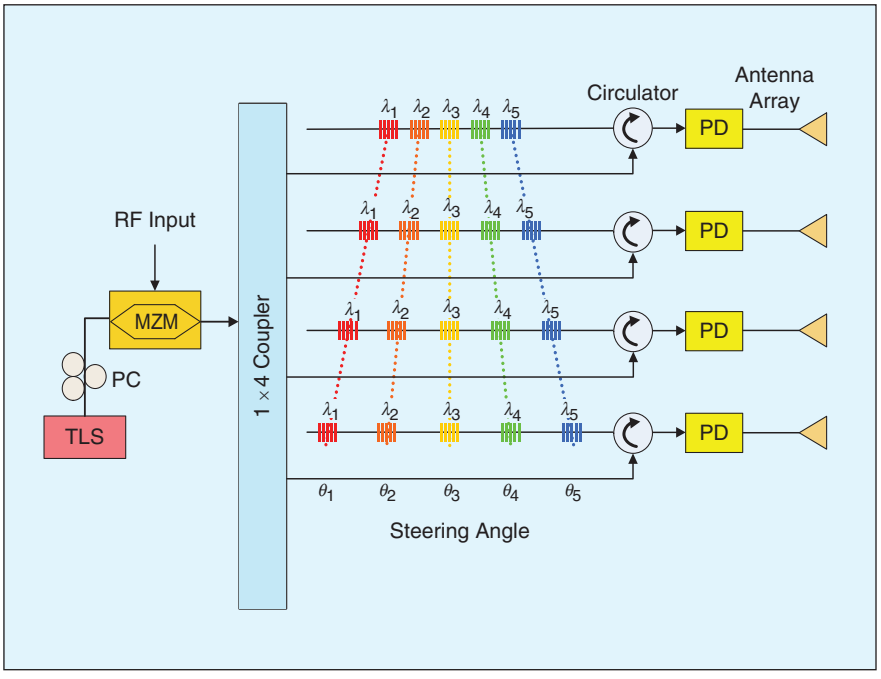

Figure 2. A photonic true-time delay beamforming system based on a FBG prism.

fiber-optic prism consisting of an array of dispersive delay lines was demonstrated in [3]. To reduce the size of the fiber-optic prism, the dispersive delay lines could be replaced by fiber Bragg grating (FBG) delay lines [4]. As an example, a FBG prism consisting of five channels of FBG delay lines is shown in Fig. 2 [5]. As can be seen the beam pointing direction can be steered by simply tuning the wavelength of the tunable laser source (TLS). If the FBG arrays in the delay lines are replaced by linearly chirped FBGs, a true-time delay beamforming system with continuous beam steering capability can be realized [6].

The architecture shown in Fig. 2 can be extended to two-dimensional (2D) beamforming [7] [8]. In [7], a 2D true-time delay beamforming system based on optical micro-electromechanical (MEMS) switches with fiber-optic delay lines

connected between cross ports was demonstrated. A 2-bit × 4-bit optical true-time delay for a 10-GHz two-dimensional phased array antenna was implemented by cascading a wavelength-dependent true-time delay unit with a unit time delay of 12 ps in the *x*-direction and a wavelength-independent true-time delay unit with a unit time delay of 6 ps in the *y*-direction.

Radio-Over-Fiber and UWB-Over-Fiber

Radio-Over-Fiber

The distribution of radio signals over optical fiber, taking advantage of the low loss and broadband bandwidth of the state-of-the-art optical fibers, has been a topic of interest for the last two decades and some radio-over-fiber (RoF) systems have been deployed for practical applications. Fig. 3 shows RoF networks that are integrated into an optical communications network for broadband wireless access. At a backbone node or a central office, baseband signals are modulated on microwave subcarriers and then modulated on an optical carrier. The signals are sent over optical fibers to base stations. Microwave signals are detected at the base stations and then radiated to free space. For uplink, microwave signals from users are received by microwave antennas at the base stations and then modulated on optical carriers, to send via the same or different optical fibers to the central office. To distribute radio signals over optical fiber a few key issues should be addressed, including 1) the dispersion-induced power fading, 2) the dynamic range and 3) the noise figure of the link. Here the first two issues will be discussed: 1) Single-sideband modulation to combat fiber chromatic dispersion, and 2) increasing dynamic range to avoid interchannel distortion.

Due to the chromatic dispersion, double-sideband modulation is not preferred in a RoF system, especially for transmission of high frequency signals over a long distance, since a double-sideband-modulated microwave signal over fiber will suffer from the chromatic-dispersion-induced power fading. The reason behind the microwave power fading along the fiber is due to the cancellation of the beat signal between the upper sideband and the carrier and the beat signal between the lower sideband and the carrier, since the optical carrier and the two sidebands will travel at different velocities, leading to the phase changes. For a RoF link using an optical fiber with a length of L and a dispersion parameter of D, the power distribution as a function of microwave frequency is given by [9]

$$P(f) = \cos^2\left(\frac{\pi LD}{C}\lambda_c^2 f^2\right) \qquad (4)$$

where λ_C is the wavelength of the optical carrier, f is the microwave frequency, C is the light velocity in vacuum.

Fig. 4 shows the microwave power of a double-sideband modulated signal as a function of the microwave frequency in a single-mode fiber of a length of 5 and 10 km. The fiber dispersion parameter is 17 ps/nm.km. Power fading due to the chromatic dispersion is clearly observed.

Although the dispersion can be compensated using a dispersion compensating fiber (DCF) or a linearly chirped FBG, a cost-effective solution is to use single-sideband modulation.

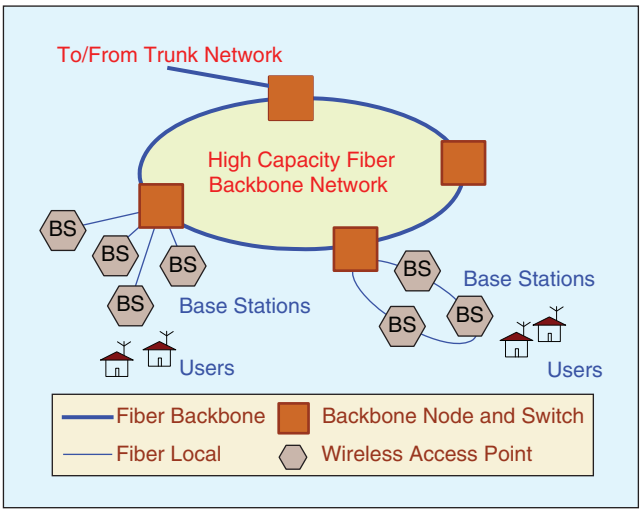

Figure 3. Convergence of wireless and fiber networks.

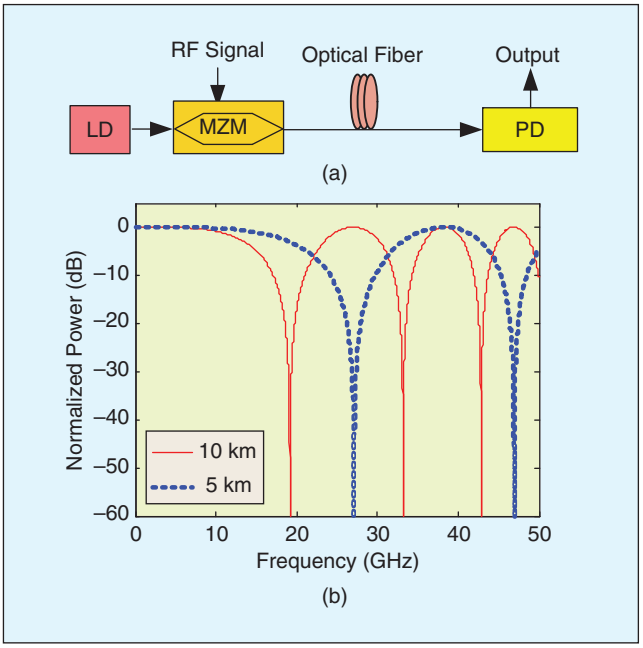

Figure 4. (a) A RoF transmission link. (b) Microwave power as a function of the microwave frequency for a given transmission length.

Fig. 5 shows the implementation of single-sideband modulation using a dual-port MZM [10]. An RF signal is applied to the two RF ports, with one being directly connected to the RF port and the other being phase shifted by 90° and then connected to the second RF port. The output signal will have the optical carrier and one optical sideband.

Single-sideband modulation can also be achieved by using an optical filter, such as an FBG or a ring resonator, to filter out one of the two sidebands [11]. The major problem associated with the approach is that the optical filter should have a narrow bandwidth to effectively suppress one of the sideband. For a microwave signal operating a low frequency (a few GHz), a regular uniform FBG can hardly fulfill this task due to the relatively large bandwidth. The use of a phase-shifted FBG that has an ultra-narrow transmission band can solve this problem [11].

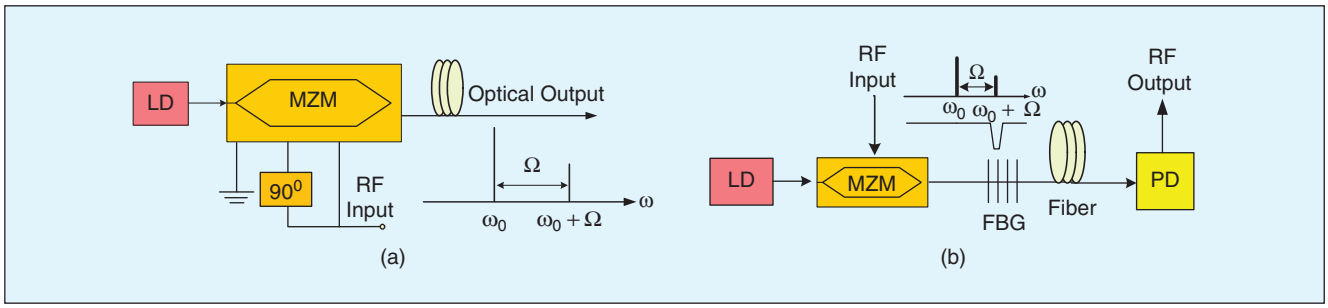

Figure 5. (a) Single-sideband modulation using a dual-port MZM. (b) Single-sideband modulation using an FBG to filter out one of the two optical sidebands.

One of the key performance measures that characterizes the performance of a RoF link is the dynamic range. In a RoF system using direct modulation or external modulation, due to the modulation nonlinearity of a LD or the inherent nonlinearity of the transfer function of a MZM, nonlinear distortions such as harmonic distortions and intermodulation distortions would be generated, which will limit the dynamic range of the RoF link. Various techniques have been proposed to combat the nonlinear distortions. It was reported in [12] that the third-order inter-modulation can be minimized in a direct-modulation-based RoF system by using an optimum bias current to the LD. The use of feed-forward linearization of a directly modulated LD would also provide a distortion cancellation [13]. The distortions of a LD can also be reduced by predistortion [14]. For a RoF system employing an external modulator, the nonlinear distortions caused by the MZM can be reduced by techniques such as predistortion of the RF signals [15] [16] and linearization of the MZM [17] [18]. In addition to the above techniques to reduce the nonlinear distortions, another solution to increase the dynamic range is to reduce the noise floor. It is known that a reduction of the noise floor would increase the spurious-free dynamic range (SFDR). Spurious-free dynamic range is defined as the difference between the minimum signal that can be detected above the noise floor and the maximum signal that can be detected without distortions (third-order intermodulation terms). In a RoF link, the SFDR is limited by several noise sources, including the optical phase-induced intensity noise, shot noise and relative-intensity noise (RIN). For a RoF link that uses independent light sources with very narrow line width, the phase-induced intensity noise is small and can be neglected. Therefore, the dominant noise sources are the shot noise and the RIN, both are associated with the average received optical power at the PD. The shot noise and the RIN powers are linearly and quadratically proportional to the received optical power. Therefore, a solution to increase the SFDR is to reduce the average received optical power. The reduction of shot noise and the RIN to improve the dynamic range of an RoF link has been proposed, such as intensity-noise cancellation [19], optical carrier filtering [20], low-biasing of a MZM [21]–[24], coherent detection [25], and optical PM-IM conversion using an FBG-based frequency discriminator [26].

UWB-Over-Fiber

As defined in Part 15 of the Federal Communications Commission (FCC) regulations [27], a UWB impulse signal should have a fractional bandwidth larger than 20% or a 3-dB bandwidth of at least 500 MHz. The UWB spectral mask defined by the FCC is shown in Fig. 6. As can be seen, the frequency band assigned to UWB indoor communications systems extends from 3.1 GHz to 10.6 GHz, with a bandwidth of 7.5 GHz centered at 7 GHz. The power density must be smaller than –41.3 dBm/MHz. Due to the low power density regulated by the FCC, the wireless transmission distance is limited

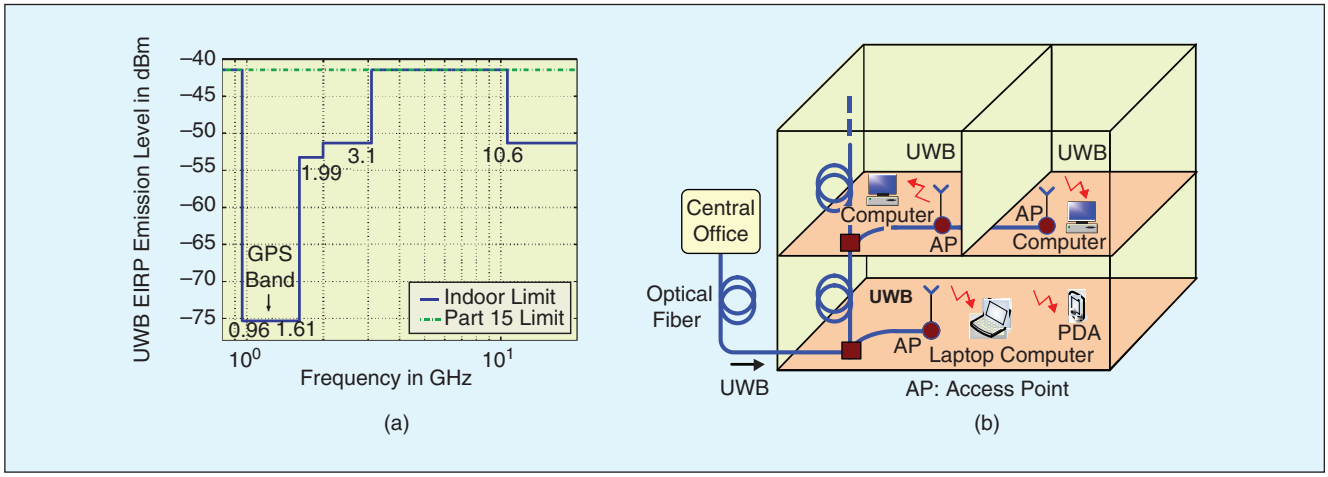

Figure 6. The UWB spectral mask defined by the FCC for UWB indoor communications. (b) UWBoF system for broadband indoor wireless access.

to a few to tens of meters. Such a short-range communications network can only operate in a standalone mode. To increase the area of coverage and to integrate the local UWB environment into fixed wired networks or wireless wide-area infrastructures, UWB signals are to be distributed using wired line such as coaxial cable or optical fiber. Thanks to the low loss and broad bandwidth of the state-of-the-art fiber, the distribution of UWB signals over fiber, or UWB-over-fiber (UWBoF) [28], is considered a promising solution. Fig. 7 shows a UWBoF system for broadband indoor wireless access. In the system, UWB signals are generated and encoded in the central office and distributed over optical fiber to the access points. At the access points, the UWB signals in the optical domain are converted to the electrical domain and then radiate to the free space. For upstream signal transmission, considering the low data-rate nature of upstream transmission, a simple and mature wireless communication technique, such as a wireless local-area network (LAN), would be used. Therefore, the entire UWBoF system would be operating in a hybrid mode to take advantage of the high-data rate feature of UWB technique for downstream signal distribution and the low cost of a mature wireless communication technique for upstream transmission.

In addition to the distribution of UWB signals over optical fiber, it is also desirable that UWB signals are generated directly in the optical domain, without the need of extra optical-electrical and electrical-optical conversions, to fully exploit the advantages provided by optics [29]. Fig. 7 shows a technique to generate UWB pulses based on phase modulation and PM-IM conversion using a FBG [30]. At the phase modulator, a Gaussian pulse is modulated on the optical carrier. By tuning the wavelength of the optical carrier to locate at the left or right linear slope of the FBG transfer function, a UWB monocycle pulse with opposite polarity is generated.

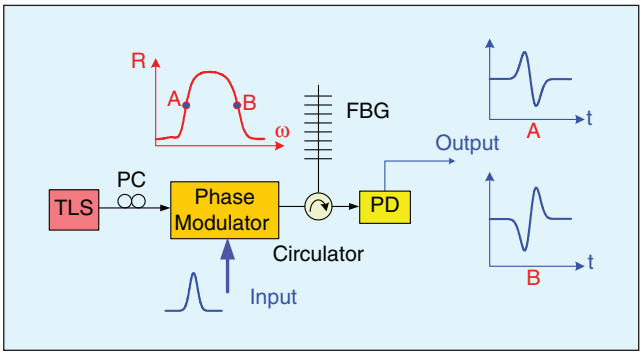

Figure 7. UWB pulse generation based on phase modulation and PM-IM conversion.

To practically deploy an UWBoF system, it is of great importance to reduce the cost. A solution is to integrate UWBoF systems into the existing wired optical access networks. Gigabit passive optical network (GPON) according to ITU-T G.984 has been widely deployed in parts of the U.S. and Europe. Meanwhile, Ethernet PON (EPON) according to the Ethernet-First-Mile standard or IEEE 802.3ah is broadly deployed in Japan and Korea. However, both GPON and EPON are based on time-division multiple access (TDMA) technology, providing services to *N* users by use of passive 1:*N* power splitters with an aggregate bit rate, so they cannot meet the requirements of future access network evolution regarding aggregated bandwidth, attainable reach and allowable power budget. Therefore, there is a worldwide consensus that the current time-division multiple access (TDMA) passive optical network would evolve toward wavelength division multiplexing PON (WDM-PON) [31]–[33]. Therefore, it is of great interest to integrate an UWBoF system into

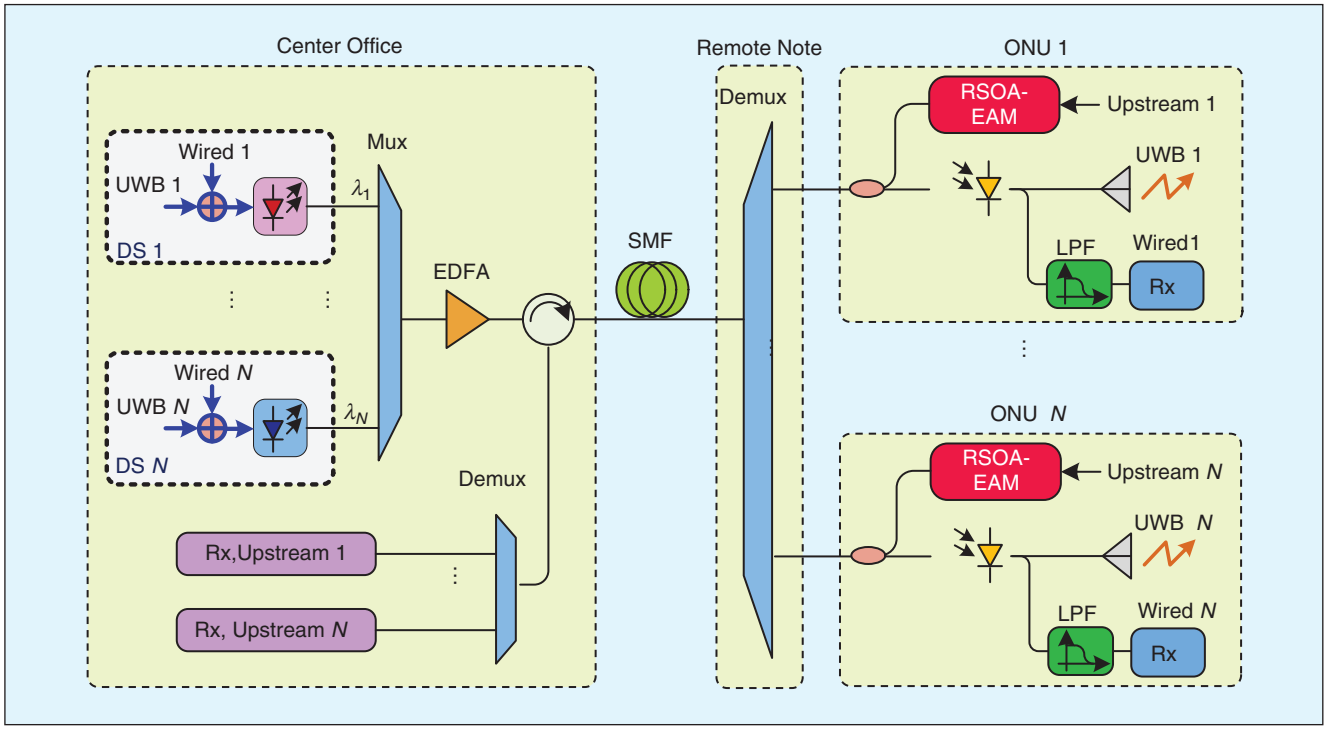

Figure 8. UWB over WDM-PON. The system is designed to provide UWB services without affecting the existing wired services.

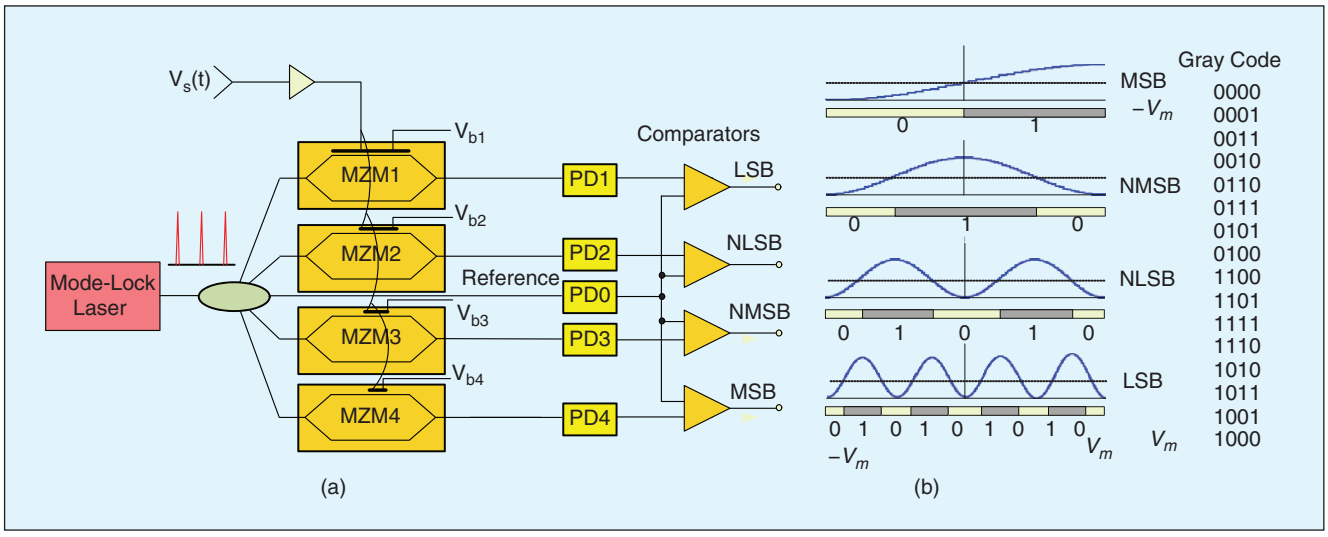

Figure 9. A 4-bit analog-to-digital converter using an array of MZMs with each modulator having an electrode length that is twice that of its nearest more significant bit. (a) The schematic of the system, (b) Gray code produced at the outputs of the comparators.

a WDM-PON network. Fig. 8 shows a UWB over WDM-PON network [34].

For downstream transmission, at the center office, a UWB signal and a baseband wired signal are combined at an electronic power combiner and then modulated on a single wavelength at a MZM. The wired signal should have a spectrum in the range of 0–3.1 GHz. Since a UWB signal, based on the spectral mark defined by the FCC, would have a spectrum in the range of 3.1–10.6 GHz, the two signals could coexist without spectral interference. The optical signal at the output of the MZM is then transmitted through a length of single-mode fiber to an optical network unit (ONU), where the optical signal is first detected by a PD and then split into two paths. In one path, the electrical signal is sent to a UWB antenna. Since a UWB antenna has a spectral response covering a range of 3.1–10.6 GHz, it can be used to act as a bandpass filter to block the wired signal. An UWBoF link is thus established. In the other path, the UWB signal is filtered out by a low-pass filter, and only the wired signal is obtained. As a result, an optical link for the wired signal transmission is implemented.

For upstream transmission, to simplify the base station, the optical carrier used for downstream transmission can be reused, which can be achieved by using a reflective semiconductor optical amplifier (RSOA). As can be seen, part of the downstream signal is tapped and sent to the RSOA. At the RSOA, the downstream signals are erased due to the gain saturation of the RSOA and the upstream signal is modulated on the same optical carrier.

In Fig. 8, the UWB signals at the central office are generated electronically and then multiplexed with the wired baseband signals. Recently, an approach to the simultaneous generation and transmission of UWB signals in the optical domain was demonstrated, which simplifies the overall system [35].

Photonics Analog-to-Digital Conversion

Analog-to-digital conversion (ADC) is essential for many applications where analog signals are digitized for processing using digital signal processing circuits. Although there is a significant progress in ADC, the sampling speed of the state-of-the-art electronics is still limited. In the last few decades, the use of optical techniques to achieve photonic ADC has attracted great interest thanks to the technological breakthrough in mode-lock laser sources, which can produce ultra-narrow and high-repetition-rate optical pulses with a timing jitter significantly below that of an electronic pulse generator. The use of optical sampling would have an added advantage of small back-coupling.

Fig. 9(a) shows a photonic analog-to-digital converter proposed by Taylor [36][37], in which an array of MZMs was used, with the input analog signal being symmetrically folded by the MZMs with each MZM having an electrode length that is twice that of its nearest more significant bit (NMSB), leading to a doubled-folding frequency, as shown in Fig. 9(b). The folding property in the transfer function imposes a requirement that the half-wave voltage of the MZM at the least significant bit (LSB) should be 2^N times lower than that of the MZM at the most significant bit (MSB), where N is the number of bit, which is difficult to realize with currently available photonics technology.

A recent solution to implement a photonic analog-to-digital converter using an array of MZMs with identical half-wave voltages was demonstrated [38]. The system architecture is identical to the one shown in Fig. 9(a), except that the MZMs are differently biased such that the transfer functions of the MZMs are laterally shifted, which leads to the generation of a linear binary code to represent the analog input signal. The operation principle is shown in Fig. 10. For an analog-to-digital converter with four channels, the four MZMs are biased with their transfer functions shifted laterally with a uniform phase spacing of $\pi/4$, as shown in Fig. 10(a). The outputs from the comparators with a threshold level as half of the full scale are shown in Fig. 10(b). The quantized values of the signal at the output of the 4-channel analog-to-digital converter are shown in Fig. 10(c). Other system structures using MZMs with identical half-wave voltages including the optical folding-flash

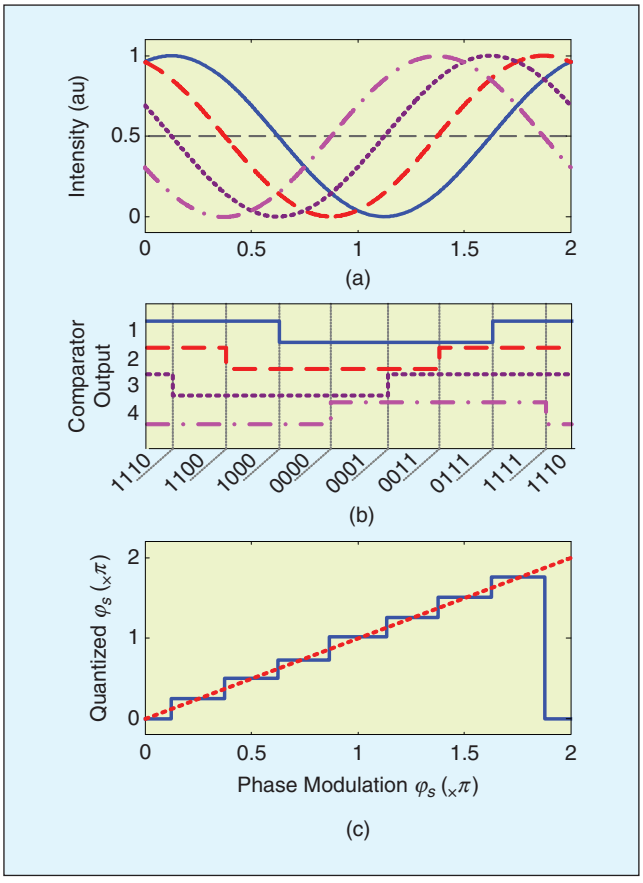

Figure 10. A 4-channel photonic analog-to-digital converter using MZMs with identical half-wave voltages. (a) The transfer functions of the four Mach-Zehnder modulators; (b) *The linear binary code* at the outputs of the comparators; (c) Quantized value (solid line) v.s. the input phase modulation (dotted line).

ADC [39] and the cascaded phase modulator-based ADC [40] were also demonstrated.

Conclusion

An overview about photonic true-time delay beamforming, radio-over-fiber and UWB-over-fiber and photonics analog-to-digital conversion was presented. The key significance of implementing these functions using photonics is the broadband width, high speed and low loss, which may not be achievable using electronics. Some of the techniques have been commercialized [41]. For example, Photonic Systems Inc. has developed a family of microwave photonic links operating over 40 GHz, offering various levels of bandwidth, noise figure and dynamic range. Pharad has developed a comprehensive family of optimized performance RF photonic transceivers for high dynamic range and low loss RF signal over optical fiber transport. OEwaves has developed ultra low phase noise microwave sources based optoelectronic oscillators for high-frequency and high performance applications. Compared with the electronic counterpart, the commercialization of microwave photonics techniques is still limited, due to the lack of photonic integrated circuits. The recent activities in photonic integrated circuits [42] would be expected to have an important impact on the development and implementation of future microwave photonics systems for both civil and defense applications.

REFERENCES

1. J. P. Yao, "A Tutorial on Microwave Photonics," *IEEE Photon. Soc. Newsletter*, vol. 26, no. 2, pp. 4–12, Apr. 2012.
2. D. Dolfi, F. Michel-Gabriel, S. Bann, and J. P. Huignard, "Two-dimensional optical architecture for time-delay beam forming in a phased-array antenna," *Opt. Lett.*, vol. 16, no. 4, pp. 255–257, Feb. 1991.
3. R. D. Esman, M. Y. Frankel, J. L. Dexter, L. Goldberg, M. G. Parent, D. Stilwell, and D. G. Cooper, "Fiber-optic prism true time-delay antenna feed," *IEEE Photon. Technol. Lett.*, vol. 5, no. 11, pp. 1347–1349, Nov. 1993.
4. H. Zmuda, R. A. Soref, P. Payson, S. Johns, and E. N. Toughlian, "Photonic beamformer for phased array antennas using a fiber grating prism," *IEEE Photon. Technol. Lett.*, vol. 9, no.2, pp. 241–243, Feb. 1997.
5. Y. Liu and J. P. Yao "Wideband true time-delay beamformer employing a tunable chirped fiber grating prism," *Appl. Opt.*, vol. 42, no. 13, pp. 2273–2277, May 2003.
6. Y. Liu, J. Yang, and J. P. Yao, "Continuous true-time-delay beamforming for phased array antenna using a tunable chirped fiber grating delay line," *IEEE Photon. Technol. Lett.*, vol. 14, no. 8, pp. 1172–1174, Aug. 2002.
7. B. M. Jung, J. D. Shin, and B. G. Kim, "Optical true time-delay for two-dimensional X-band phased array antennas," *IEEE Photon. Technol. Lett.*, vol. 19, pp. 877–879, Jun. 2007.
8. B. M. Jung and J. P. Yao, "A two-dimensional optical true time-delay beamformer consisting of a fiber Bragg grating prism and switch-based fiber-optic delay lines," *IEEE Photon. Technol. Lett.*, vol. 21, no. 10, pp. 627–629, May 2009.
9. G. H. Smith, D. Novak, and Z. Ahmed, "Overcoming chromatic-dispersion effects in fiber-wireless systems incorporating external modulators," *IEEE Trans. Microwave Theory Tech.,* vol. 45, no. 8, pp. 1410–1415, Aug. 1997.
10. J. Park, W. V. Sorin, and K. Y. Lau, "Elimination of the fibre chromatic dispersion penalty on 1550 nm millimeter-wave optical transmission," *Electron. Lett.*, vol. 33, no. 6, pp. 512–513, Mar. 1997.
11. S. Blais and J. P. Yao, "Optical single sideband modulation using an ultranarrow dual-transmission-band fiber Bragg grating," *IEEE Photon. Technol. Lett.*, vol. 18, no. 21, pp. 2230–2232, Nov. 2006.
12. S. Yaalob, W. R. Wan Abdullah, M. N. Osman, A. K. Zamzuri, R. Mohamad, M. R. Yahya, A. F. Awang Mat, M. R. Mokhtar, and H. A. Abdul Rashid, "Effect of laser bias current to the third order intermodulation in the radio over fibre system," *RF and Microwave Conference*, Sept. 2006, pp. 444–447.
13. D. Hassin and R.Vahldieck, "Feedforward linearization of analog modulated laser diodes—Theoretical analysis and experimental verification," *IEEE Trans. Microw. Theory Tech.*, vol. 41, no. 12, pp. 2376–2382, Dec. 1993.

14. L. Roselli, V. Borgioni, F. Zepparelli, F. Ambrosi, M. Comez, P. Faccin, and A. Casini, "Analog laser predistortion for multiservice radio-over-fiber systems," *J. Lightw. Technol.*, vol. 21, no. 5, pp. 1211–1223, May 2003.
15. A. Katz, W. Jemison, M. Kubak, and J. Dragone, "Improved radio over fiber performance using predistortion linearization," in *IEEE MTT-S Int. Microw. Symp. Dig.*, Philadelphia, PA, Jun. 2003, pp. 1403–1406.
16. V. Magoon and B. Jalali, "Electronic linearization and bias control for externally modulated fiber optic link," in *IEEE Int. Microw. Photon. Meeting*, Oxford, U.K., Sep. 2000, pp. 145–147.
17. J. H. Schaffner and W. B. Bridges, "Inter-modulation distortion in high dynamic range microwave fiber-optic links with linearized modulators," *J. Lightw. Technol.,* vol. 11, no. 1 pp. 3–6, Jan. 1993.
18. E. I. Ackerman, "Broad-band linearization of a Mach–Zehnder electrooptic modulator," *IEEE Trans. Microw. Theory Tech.*, vol. 47, no. 12, pp. 2271–2279, Dec. 1999.
19. S. Mathai, F. Cappelluti, T. Jung, D. Novak, R. B. Waterhouse, D. Siveco, A. Y. Cho, G. Ghione, and M. C. Wu, "Experimental demonstration of a balanced electroabsorption modulated microwave photonic link," *IEEE Trans. Microw. Theory Tech.*, vol. 49, no. 10, pp. 1956–1961, Oct. 2001.
20. R. D. Esman and K. J. Williams, "Wideband efficiency improvement of fiber optic systems by carrier subtraction," *IEEE Photon. Technol. Lett.*, vol. 7, no. 2, pp. 218–220, Feb. 1995.
21. T. E. Darcie, and P. F. Driessen, "Class-AB Techniques for high-dynamic-range microwave photonic links," *IEEE Photon. Technol. Lett.*, vol. 18, no. 8, pp. 929–931, Apr. 2006.
22. L. T. Nichols, K. J. Williams, and R. D. Esman, "Optimizing the ultrawide-band photonic link," *IEEE Trans. Microw. Theory Tech.,* vol. 45, no. 8, pp. 1384–1389, Aug. 1997.
23. M. L. Farwell, W. S. C. Chang, and D. R. Huber, "Increased linear dynamic range by low biasing the Mach–Zehnder modulator," *IEEE Photon. Technol. Lett.,* vol. 5, no. 7, pp. 779–782, Jul. 1999.
24. T. E. Darcie, A. Moye, P. F. Driessen, J. D. Bull, H. Kato, and N. A. F. Jaeger, "Noise reduction in class-AB microwave-photonic links," in *International topical meeting on Microwave Photonics* (Seoul, South Korea, 2005), pp. 329–332.
25. C. Lindsay, "An analysis of coherent carrier suppression for photonic microwave links," *IEEE Trans. Microw. Theory Tech.,* vol. 47, no. 7, pp. 1194–1200, Jul. 1999.
26. Y. Yan and J. P. Yao, "Photonic microwave bandpass filter with improved dynamic range," *Opt. Lett.*, vol. 33, no. 15, pp. 1756–1758, Aug. 2008.
27. L. Yang, and G. B. Giannakis, "Ultra-wideband communications: an idea whose time has come," *IEEE Signal Processing Mag.,* vol. 21, no. 6, pp. 26–54, Nov. 2004.
28. J. P. Yao, F. Zeng, and Q. Wang, "Photonic generation of Ultra-Wideband signals," *J. Lightw. Technol.,* vol. 25, no. 11, pp. 3219–3235, Nov. 2007.
29. J. P. Yao, F. Zeng, and Q. Wang, "Photonic generation of Ultra-Wideband signals," *J. Lightw. Technol.,* vol. 25, no. 11, pp. 3219–3235, Nov. 2007.
30. F. Zeng and J. P. Yao, "Ultrawideband impulse radio signal generation using a high-speed electrooptic phase modulator and a fiber-Bragg-grating-based frequency discriminator," *IEEE Photon. Technol. Lett.,* vol. 18, no. 19, pp. 2062–2064, Oct. 2006.
31. K. Grobe and J. P. Elbers, "PON in adolescence: From TDMA to WDM-PON," *IEEE Commun. Mag.,* vol. 46, no. 1, pp. 26–34, Jan. 2008.
32. F. Ponzini, F. Cavaliere, G. Berrettini, M. Presi, E. Ciaramella, N. Calabretta, and A. Bogoni, "Evolution scenario toward WDM-PON," *J. Opt. Commun. Netw.,* vol. 1, no. 4, pp. C25–C34, Sep. 2009.
33. G. K. Chang, A. Chowdhury, Z. S. Jia, H. C. Chien, M. F. Huang, J. J. Yu, and G. Ellinas, "Key technologies of WDM-PON for future converged optical broadband access networks," *J. Opt. Commun. Netw.,* vol. 1, no. 4, pp. C35–C50, Sep. 2009.
34. S. Pan and J. P. Yao, "Simultaneous provision of UWB and wired services in a WDM-PON network using a centralized light source," *IEEE Photon. J.,* vol. 2, no. 5, pp. 712–718, Oct. 2010.
35. S. Pan and J. P. Yao, "Provision of IR-UWB wireless and baseband wired services over a WDM-PON," *Opt. Express,* vol. 19, no. 26, pp. B209–B217, Dec. 2011.
36. H. F. Taylor, "An electrooptic analog-to-digital converter," *Proc. IEEE,* vol. 63, no. 10, pp. 1524–1525, Oct. 1975.
37. H. F. Taylor, "An optical analog-to-digital converter-design and analysis," *IEEE J. Quantum Electron.,* vol. 15, no.4, pp. 210–216, Apr. 1979.
38. H. Chi and J. P. Yao, "A photonic analog-to-digital conversion scheme using Mach-Zehnder modulators with identical half-wave voltages," *Opt. Express,* vol. 16, no. 2, pp. 567–572, Jan. 2008.
39. B. Jalali and Y. M. Xie, "Optical folding-flash analog-to-digital converter with analog encoding," *Opt. Lett.,* vol. 20, no. 18, pp. 1901–1903, Sep. 1995.
40. M. Currie, "Optical quantization of microwave signals via distributed phase modulation," *J. Lightwave Technol.,* vol. 23, no. 2, pp. 827–833, Feb. 2005.
41. Technology Focus: Microwave photonics, Nature Photon. vol. 5, no. 12, Dec. 2011.
42. L. A. Coldren, "Photonic Integrated Circuits for microwave photonics," *2010 IEEE Topical Meeting on Microwave Photonics*, pp. 1–4, Oct. 2010.